Fuel supply optimization in micro fuel cells

Ai Kamitani, Satoshi Morishita, Hiroshi Kotaki, S. Arscott

Available online at www.sciencedirect.com
ScienceDirect
Procedia Chemistry 1 (2009) 457–460
Procedia Chemistry
www.elsevier.com/locate/procedia

Proceedings of the Eurosensors XXIII conference

Fuel supply optimization in micro fuel cells

Ai Kamitani[a], Satoshi Morishita[a], Hiroshi Kotaki[a] and Steve Arscott[b]

[a]*Advanced Technology Research Laboratories, SHARP Corp., Nara, Japan.*
[b]*Institute of Electronics, Microelectronics and Nanotechnology (IEMN) , Centre National de la Recherche Scientifique (CNRS), University of Lille, Villeneuve d'Ascq, France.*

Abstract

Miniature high-performance micro fuel cells (µFC) operating at room temperature have been fabricated using microsystems technologies. The smallest µFCs have a reaction surface of 0.11 cm^2 (volume ~18.6 mm^3; mass ~35.6 mg) and produce an output power density of 22.9 mW/cm^2. The insertion of a hydrophilic macroporous layer into the anode diffusion layer stack, an input fuel flow rate as low as 550 nL min^{-1} produces 9.25 mW/cm^2 at a fuel use efficiency of ~75%. By optimizing the microfluidic architecture, e.g. the microchannel dimensions and the diffusion layer stack, we demonstrate of the smallest, highest performance µFCs reported to date.

Keywords: energy; micro fuel cell; microsystem; integration; MEMS; silicon

1. Introduction

Micro fuel cells (µFC)[1] have the potential for powering a multitude of portable electronic systems, e.g. mobile phones, laptops, media players, personal organizers etc. They could also be harnessed for on-chip energy sources for future autonomous micro and nano-electromechanical systems (MEMS/NEMS); integration of these microsystems with silicon microelectronics would be highly desirable for a whole range of future sensors and actuators based on micro and nanosystems technologies. Methanol fuel µFCs[2] are being studied for several reasons *inter alia*: a high energy density (4.3 $kWhL^{-1}$), the storage benefits of a liquid fuel, the possibility of on-chip integration and subsequent batch production. High performance miniaturized µFCs will be achieved by optimization of the mass transport issues[3] such as cross-over, water and carbon dioxide management and fuel concentration. By applying microfluidic technologies to form microchannels[4] for µFC fabrication by making use of microsystems fabrication processes[5,6] the above issues can be addressed.

The goal of this paper is to optimize the fuel (aqueous methanol solution) supply to the anode of a µFC. We have studied very small surface µFCs (0.11 cm^2) and very low fuel flow rates (550 nL min^{-1}). We have also modified the diffusion layer stack at the anode to include a novel hydrophilic macroporous layer; we have observed that the fuel use efficiency can be significantly boosted by this modification. It is important to state that our observations and conclusions are by no means unique to methanol fuel µFCs but could be applied to other liquid-fuel µFCs based on e.g. bio-ethanol, glucose solution etc.

*corresponding author: steve.arscott@iemn.univ-lille1.fr

doi:10.1016/j.proche.2009.07.114

2. Cell design

The two basic µFC structures studied here are shown in Figure 1. Serpentine microchannels were used for the anode and the cathode. The anode microchannels had a height of 100 µm and a width of 50 µm; the cathode microchannels had a height of 150 µm and a width of 200 µm. In order to vary the area of the µFC the length of the microchannel was varied from 3 cm (A_{FC} = 0.11 cm^2) to 12 cm (A_{FC} =0.39 cm^2). In order to investigate a possible optimization of the anode diffusion layer stack we modified the µFC set-up [see Fig. 1(b)] to include a macroporous layer [see Fig. 4(a)]; the fuel and air flow patterns will be discussed later in the performance section of the paper.

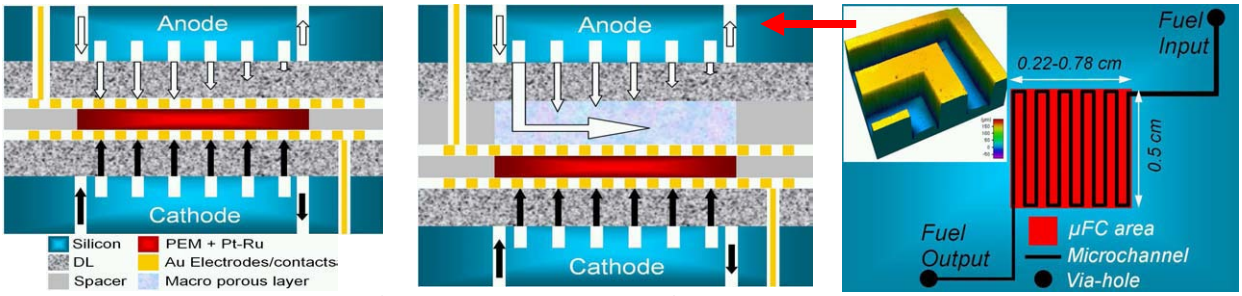

Fig. 1(a) µFC using microchannels (b) modified µFC [*white (black) arrows = fuel (air)*] (c) anode architecture (inset = a 3D microscope image)

3. Microfabrication and set-up

The microfabrication process[5] uses silicon wafers to fabricate the microchannels for the anode and the cathode, see Fig. 2(a). There are 3 main phases: (i) via-holes fabrication for the microfluidic/gas connections and the electrical contacts, (ii) fabrication of the microchannels and (iii) surface modification. Following photolithography, the silicon wafer is etched to form the via-holes using a successive etch/passivation DRIE in a plasma etcher (STS, UK). Lithography is used define the microchannels on the wafer surfaces; see Fig. 2(b). Lithography protects the anode microchannels whilst a hydrophobic fluorocarbon layer is deposited onto the wafer surface. A fluorocarbon layer is also deposited onto cathode wafer; no masking was used to protect the cathode microchannels which were rendered hydrophobic. The measurement set-up is shown in Fig. 2(c); details of which are published elsewhere[5,6].

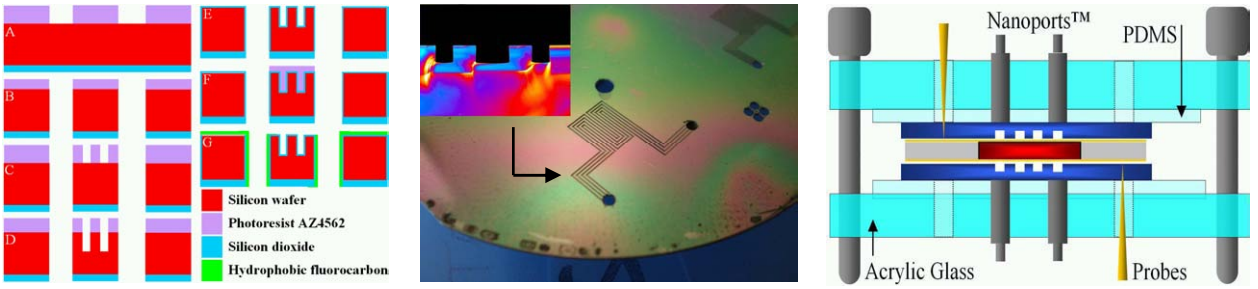

Fig. 2(a) Fabrication steps (b) DRIE microchannels (inset = microchannel cross-section) (c) set-up rig developed for tests

4. Cell performance

4.2 Variation of fuel cell surface

Cell performances were judged in terms of maximum output power density P_{max} (mW cm^{-2}) and fuel use efficiency (FUE) which is a figure of merit[7] relating to the current density (mW cm^{-2}) at P_{max}, the active cell surface A_{FC} (cm^2) ad the fuel flow rate (mol s^{-1}). Figure 3 shows the output power density of fuels cells having a surface area equal to 0.11 cm^2, 0.18 cm^2 and 0.39 cm^2 as a function of fuel flow rate (air flow rate at a constant 30 sccm; oxygen supply is ensured over the whole cathode surface[5]); the tests were made using the basic cell set-up c.f. Fig. 1(a). Fig. 3(a) shows results obtained using the smallest area fuel cell; a room temperature P_{max} of 22.9 mW cm^{-2} was measured for a fuel cell having an active area equal to 0.11 cm^2 at a fuel flow rate of 8.28 µL min^{-1}. At a lower flow rate of 1.38 µL min^{-1} P_{max} falls to 11 mW cm^{-2}. P_{max} is only 5.8 mW cm^{-2} at 8.28 µL min^{-1} for the largest cell. First,

P_{max} is inversely proportional to A_{FC} at a given flow rate. A power density saturation effect is present in the smallest cell not observed in the larger cell; this is indicative of a lack of fuel supply to the entire surface for the largest cell, a much larger fuel flow rate (>10µL min^{-1}) would be required to achieve a P_{max} observed for the smallest cell.

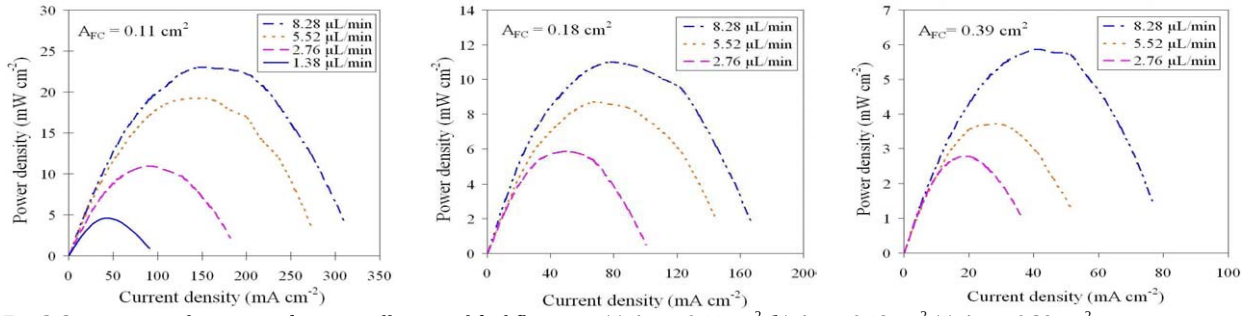

Fig. 3 Output power density as a function cell area and fuel flow rate: (a) A_{FC} = 0.11 cm^2 (b) A_{FC} = 0.18 cm^2 (c) A_{FC} = 0.39 cm^2.

4.3 Inclusion of anode hydrophilic macroporous layer

Figure 4 shows results obtained when including a hydrophilic macroporous layer using modified set-up shown in Fig. 1(b). A P_{max} of 12.7 mW/cm^2 was obtained at a FUE of 20%. The P_{max} of the 0.25 cm^2 µFC, without the macro porous layer, is 4.8 mW cm^{-2} at 550 nL min^{-1}. In contrast, inclusion of the macroporous layer into the µFC anode stack yields a P_{max} of 9.25 mW cm^{-2}; a ~2 fold increase. More striking, the observed P_{max} of 9.25mW/cm^2 is achieved at a mere 550 nL/min (FUE = 75.4%). This macroporous layer promotes capillary filling via wicking and a subsequent uniform fuel distribution over the anode catalyst layer and we believe[6] also promotes the removal of CO_2 bubbles from the anode catalyst layer due to its hydrophilic nature where bubble detachment from the anode catalyst layer is promoted. Optical microscopy of fuel filling [using colour dyes: see Fig. 4(c)] revealed that liquid fuel flow can occur along fibres; the pores between fibres could allow the promotion of carbon dioxide removal.

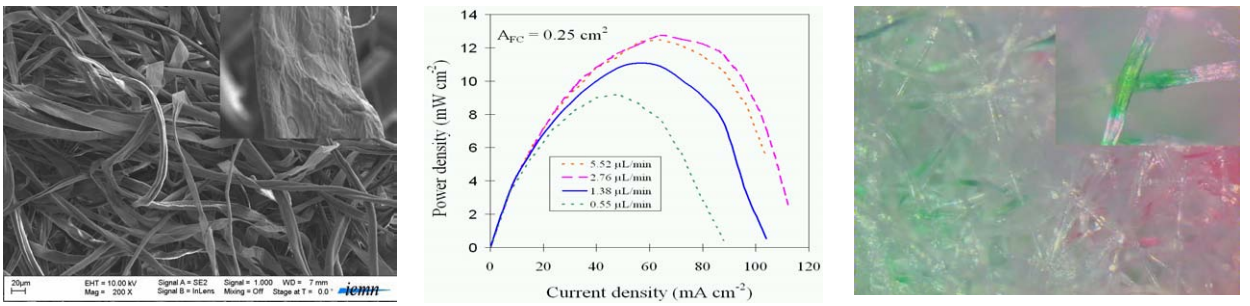

Fig. 4 (a) SEM image of macroporous layer (inset = zoom ×10) (b) power density with macroporous layer (b) fuel filling of macroporous layer

Figure 5 shows a tabular summary of our results presented in this paper.

A_{FC} (cm^2)	Vol. (mm^3)	Mass (mg)	P_{max} (mW/cm^2)	FUE %
0.39	65.9	126.4	2.45	15
0.3[a]	50.7	97.2	4.3	20.1
0.25[b]	42.3	81	6.4	22.5
0.25[c]	48.3	82.8	11.1	35.1
0.18	30.4	58.3	2	11.7
0.11	**18.6**	**35.6**	4.47	12.4

A_{FC} (cm^2)	J (mA/cm^2)	P_{max} (mW/cm^2)	P_{max} (mW/cm^3)	FUE %
0.39	20.5	2.6	16.6	10
0.3[a]	47	7.9	46.7	17.7
0.25[b]	40	8	47.3	12.5
0.25[c]	64	12.7	65.8	20
0.25[c,d]	48	9.25	47.9	**75.4**
0.18	50	5.8	34.3	11.3
0.11	91	11	65.1	12.5
0.11[e]	164	**22.9**	**135.5**	7.5

Fig. 5 Summary of results obtained from all µFCs tested. Table I: fuel flow rate = 1.38 µL min^{-1} unless stated; table II fuel flow rate = 2.76 µL min^{-1} unless stated. Notable numbers are given in bold. Superscripts a-e refer to: (a) anode microchannel height = 50 µm (b) macroporous layer not included (c) macroporous layer included (d) fuel flow rate = 550 nL/min (e) fuel flow rate = 8.28 µL/min

A short microchannel implies a small surface; the whole surface can be supplied with fuel at a low flow rate; this leads to a high P_{max} at a low flow rate. Nothing is gained by increasing the flow rate further as P_{max} saturation is observed [see Fig. 3(a)] and the result is a reduction in the FUE; In this case, a short microchannel (small cell area) does not imply a low absolute power output ($A_{FC} \times P_{max}$). For example, the smallest cell produces 2.5 mW of absolute power, whereas the largest cell produces 2.3 mW. In contrast, a long microchannel (large cell area) achieves a comparable absolute power which results from poor fuel supply to the whole anode surface (unless at very high flow rates [larger than used here >10 µL min^{-1}] where leaks can occur and a reduction in the FUE would occur). The fact that we observe a slightly improved FUE for a larger cell (at a fuel flow rate of 8.28 µL min^{-1}) is probably explained by the increase of pressure inside the cell which promotes fuel diffusion to the anode; this assumption is backed up by the fact that by reducing the microchannel height (see Fig. 5) one also observes an increase in P_{max}; increasing the microchannel length and reducing the microchannel height leads to an increase in the hydrostatic pressure in the cell. Interestingly, the values of the FUE for the smallest and the largest cells (without macroporous layer) are approximately the same; only the inclusion of the hydrophilic macroporous layer into the anode stack drastically improves the FUE. An important figure to note is the very respectable >100 mW per cubic centimetre expected from an imaginary "stack" of the smallest cells working in parallel; such a figure is compatible with performances requirements for autonomous MEMS currently under reasearch[8]. We note also that our results compare very favourably in terms of P_{max} and FUE to recent state-of-the-art work on similar µFCs published in the litterature[9-12].

5. Conclusions

Microsystems technologies are shown to be useful for producing very tiny micro fuel cells having a surface area as small ~0.1 cm^2 capable of producing a room temperature P_{max} >20 mW/cm^2. The study showed that improved cell performances in terms of power density can be achieved at low flow rates (<10 µL min^{-1}) by reducing the fuel cell area and by modifying the anode diffusion layer stack. In the latter case, the insertion of a highly absorbent hydrophilic macroporous layer into the anode stack drastically improved the fuel use efficiency by maintaining a relatively high power output (~9 mW cm^{-2}) at reduced fuel flow rates (<1 µL/min) and room temperature. The maximum power density output can effectively be increased by a factor of ~2 via the inclusion of the hydrophilic layer; we interpret this as equalization of the methanol concentration over the whole anode catalyst layer surface ensuring that the fuel needs of the anode are met at reduced fuel flow rates and promotion of CO_2 bubble removal.

Acknowledgements

The authors would like to thank Dr T. Chiba and Dr A. Takahashi from SHARP Corporation and Professor A. Cappy (Head of IEMN) for their support of the project.

References

1. Steele B C H, Heinzel A. Materials for fuel-cell technologies. *Nature* 2001;**414**:345-352.
2. Arico A S, Srinivasan S, Antonucci V. DMFCs: From fundamental aspects to technology development. *Fuel Cells* 2001;**1**:133-161.
3. Scott K, Taama WM, Argyropoulos P, Sundmacher K. The impact of mass transport and methanol crossover on the direct methanol fuel cell. *J. Power Sources* 1999;**83**:204–216.
4. Carlier J, Arscott S, Thomy V, Fourrier JC, Caron F, Camart JC, Druon C, Tabourier P. Integrated microfluidics based on multi-layered SU-8, *J. Micromech. Microeng*. 2004;**14**:619–624.
5. Kamitani A, Morishita S, Kotaki H, Arscott S. Miniaturized microDMFC using silicon microsystems techniques. *J. Micromech. Microeng.* 2008;**18**:125019-28
6. Kamitani A, Morishita S, Kotaki H, Arscott S. Improved fuel use efficiency in microchannel direct methanol fuel cells using a hydrophilic macroporous layer, *J. Power Sources* 2009;**187**:148–155
7. O'Hayre R. *Fuel Cell Fundamentals*. New York: John Wiley & Sons; 2006.
8. Dargent T, Bao XQ, Grondel S, Le Brun G, Paquet JB, Soyer C, Cattan E. Micromachining of an SU-8 flapping-wing flying MEMS *J. Micromech. Microeng*. 2009 (to be published)
9. Yen TJ, Fang N, Zhang X, Lu GQ, Wang CY. A micro methanol fuel cell operating at near room temperature *Appl. Phys. Lett*. 2003;**83**:4056–4058
10. Wozniak K, Johansson D, Bring M, Sanz-Velasco A, Enoksson P. A micro direct methanol fuel cell demonstrator *J. Micromech. Microeng.* 2004;**14**:S59–S63.
11. Liu X, Suo C, Zhang Y, Wang X, Sun C, Li L, Zhang L. Novel modification of Nafion117 for a MEMS-based micro direct methanol fuel cell (μDMFC) *J. Micromech. Microeng*. 2006;**16**:S226–S232.
12. Esquivel JP, Sabate N, Santander J, Torres N, Cane C. Fabrication and characterization of a passive silicon-based direct methanol fuel cell *Microsyst. Technol*. 2008 ;**14**:535–541.